CONF-910931--2

IS-M--674

DE92 001764

SCALING ANALYSIS OF SURFACE ROUGHNESS IN SIMPLE MODELS FOR MOLECULAR-BEAM EPITAXY*

H. C. Kang† and J. W. Evans§

Departments of Chemistry† and Mathematics§, and Ames Laboratory,
Iowa State University, Ames, Iowa 50011

ABSTRACT:

There is currently interest in simple models for Molecular-Beam Epitaxy (MBE) which mimic the effect of thermal mobility by allowing incorporation of deposited atoms at kink sites within a distance l of the deposition site. Scaling of the interface width, W, with mean film height, $\langle h \rangle$, of the form $W \sim \langle h \rangle^{\beta}$, is analysed. Studies for a Solid-on-Solid geometry in d=1+1 dimensions revealed a sudden transition from the T=0 K (l=0) behavior of $\beta = 1/2$ to a new universality class for $l \geq 1$ with β=3/8. We consider the effect of incorporating realistic adsorption-site geometries and deposition dynamics into these d=1+1 MBE models. We find that β is always less than 3/8 at T =0 K (l=0) due to lateral coupling, and that the effective β increases smoothly with smaller l at least to 3/8. However, for larger l, the simple scaling of W described above breaks down in the physically relevant range of $\langle h \rangle$.

† Present address: Department of Chemistry, National University of Singapore, Kent Ridge, Singapore 0511

* Submitted for the Proceedings of the 12th European Conference on Surface Science, Stockholm, Sweden Sept 9-12 1991.

1. INTRODUCTION.

There has been much interest in the scaling of the interface width, $W = \langle (h-\langle h \rangle)^2 \rangle^{1/2}$, in microscopic (lattice) models for far-from-equilibrium film growth (1). Here h is the height variable, and $\langle h \rangle$ denotes the mean film height in monolayers, say. Specifically, one looks for scaling of the form $W \sim \langle h \rangle^{\beta}$ (or t^{β} where t denotes time). Models usually fall into a few distinct "dynamic universality classes" characterized by different scaling exponents, ß.

Recently a simple model was proposed for Molecular-Beam Epitaxy (MBE), in which the key effect of thermally-activated surface mobility is to allow adatom migration to and incorporation at nearby kink sites (2, 3). Simulations for a Solid-on-Solid (SOS) geometry in d=1+1 dimensions showed that as temperature, T, increased, so kink migration was activated, ß shifted from the T = 0 K value of 1/2 to a value around 3/8 for a range of T, before finally moving lower (3). The value $\beta=3/8$ represents a new universality class. This new universality class was also achieved in simplified SOS models, where deposited atoms were incorporated immediately after deposition at the nearest kink site within a distance l of the deposition site. For these models, the "effective" ß assumed a value of 3/8, essentially independent of $l \geq 1$ (2,3). (The "true" asymptotic value might differ.)

Here we consider analogous MBE models incorporating kink migration for a more realistic choice of adsorption site geometry and deposition dynamics (4). Of course, the on-top-site adsorption in the SOS geometry is unrealistic. Importantly for this discussion, the associated deposition models suffer from an unphysical lack of lateral coupling in the T = 0 K limit. This is what allows the rapid transition described above to the new universality class. For realistic adsorption site geometries and deposition dynamics, we show that the T = 0 K value of ß is always less than 3/8, and "effective" β increases smoothly from this value with increasing l. However for larger l, W does not satisfy the simple scaling described above for the physically relevant range of $\langle h \rangle$ of 10^1-10^3.

2. MBE MODELS AND THEIR COARSE-GRAINED EVOLUTION EQUATIONS.

Here we consider only the simplified MBE models (2,3) where an atom after deposition migrates immediately to the nearest kink site within a distance l. If a particle arrives at a kink site within the same level, it sticks there; if it arrives at a cliff edge, it sticks at the kink site at the bottom of the cliff. If there are two equidistant nearest kink sites or cliff edges, one is chosen at random. If there are none within a distance l, the particle stays where it was deposited. The model A, say, considered previously (2,3) for random deposition at on-top sites in an SOS geometry is shown in Fig. 1a. Here we consider the analogous model B, shown in Fig. 1b, for random deposition (i.e., addition with equal probability) at bridge sites. This mimics a more realistic adsorption site geometry, but not deposition dynamics. Finally we consider a model C , shown in Fig. 1c, where atoms impinge randomly at all points on the surface and are funneled downward to the nearest bridge site. This mimics a realistic adsorption site geometry and deposition dynamics (with sticking coefficient of unity) at least for metal-on-fcc(100) metal epitaxy (4). As described above, immediately after deposition the kink site migration algorithm is applied in all cases.

In a coarse-grained description of these models, one postulates that the evolution of the interface height, h(x,t) at position x and time t, is described by a stochastic differential equation of the form (cf. Ref. 1-3):

$$\partial h/\partial t = R(\nabla h, \nabla^2 h, \ldots) - \nabla \cdot j_{eq} + \eta \qquad (1)$$

Here η denotes the noise which produces surface roughness. It is assumed to have zero mean and to be delta-function correlated in space and time. Next, j_{eq} denotes flux from mass-conserving thermal diffusion processes (5,6). It is taken to have the form

$$j_{eq} = \kappa_{eq}\nabla(\nabla^2 h) + \lambda_{eq}\nabla(\nabla h)^2 + \ldots \quad (2)$$

The first term in Eq. 2 has the standard Mullins form (7) for surface diffusion, and the second is a relevant nonlinear correction (2,6). There is no $-\nu_{eq}\nabla h$ term, in the absence of a thermal (or gravitational) driving force for downward motion (2,5). Finally, the term R in Eq. 1 has the form

$$R = J\,S(\nabla h, \nabla^2 h, \ldots)/\rho - \nabla\cdot j_{ne} \quad (3)$$

and characterizes growth due to the non-equilibrium deposition dynamics alone, for example at T = 0 K (cf. Ref. 8).. Here J denotes the deposition flux, ρ the film density (which is constant if there are no defects), S the sticking coefficient, and j_{ne} represents any surface flux during deposition. The sticking coefficient, S, is typically unity in real systems and thus independent of ∇h, $\nabla^2 h$, etc.. This is the case in models A and C depicted in Fig. 1. In model A, one also has $j_{ne} = 0$. However in model C, there is a downward flux $j_{ne} \propto -J\nabla h/\rho$ due to funneling. It is also instructive to consider the less-physical case of model B. Here $j_{ne} = 0$ and S is proportional to bridge site density, so S decreases with mean slope (9) and is larger (smaller) at local minima (maxima). In summary, R always has the form

$$R = \nu_0 + \lambda(\nabla h)^2/2 + \nu\nabla^2 h + \ldots$$

with λ non-zero only in model B , and ν zero only in model A. The third term, $\nu\nabla^2 h$, reflects lateral coupling due to realistic adsorption site geometries and deposition dynamics (Figs. 1b and c). *We emphasize that it is only for the unphysical SOS adsorption site geometry that one can set $\nu = 0$.*

3. RESULTS FOR d=1+1 MBE MODELS.

Previous results for the d=1+1 MBE model A with SOS geometry (2,3) can be understood noting the slope-independence of the growth velocity ($\lambda = 0$), and the artificial lack of lateral coupling in the deposition dynamics ($\nu = 0$). A straightforward Fourier analysis of the linear equation

$$\partial h/\partial t = v_0 + \kappa_{eq}\nabla^2(\nabla^2 h) + \eta \qquad (4)$$

produces $\beta = 3/8$ (2,3). This was seen for all models with $l \geq 1$ (2,3). The nonlinear quartic term in Eq. 2 is also relevant to the asymptotic behavior. It has been argued that it must eventually dominate (2), leading to a crossover to a universality class with $\beta = 1/3$ (6). This was not seen in the simulations of model A.

Here we present Monte-Carlo simulation results for d=1+1 MBE models B and C starting from a large perfect substrate of fixed size (10000 sites) with periodic boundary conditions. Films are grown to a mean height of 4000 monolayers. We obtain accurate statistics by averaging over 50 growth trials. Specifically, the local slope of ln W versus ln <h>, i.e., the local β, can be determined essentially exactly. However we shall see that these curves can be non-linear, and the asymptotic β is difficult to determine precisely (as usual).

For the d=1+1 MBE model B incorporating random deposition at bridge sites, one has $\lambda < 0$ and $\nu > 0$ (9) so standard Kadar-Parisi-Zhang (KPZ) behavior should apply, with $\beta = 1/3$ (1, 4, 9). Indeed, this is observed in our MBE simulations for $l = 0$ (T = 0 K). As l increases, the effective β increases smoothly but rapidly to values even beyond 3/8 (Table 1). This no doubt corresponds to κ_{eq} increasing, but λ and ν remaining fixed, as l increases. However it should be emphasized that for $l \geq 10$ one finds that simple scaling for W breaks down in the physically relevant range of <h>

of 10^1-10^3 (Fig. 2).

Finally, for the most realistic d=1+1 MBE model, C, with downward-funneling to bridge sites (4), one finds $\lambda = 0$ but $\nu > 0$, so standard Edwards-Wilkinson (EW) behavior should apply with $\beta = 1/4$ (1,4). Again, this is observed in our simulations for $l = 0$ (T = 0 K). Here the effective β increases smoothly with l to about 3/8 when $l = 20$ (Table 1). Presumably κ_{eq} is increasing, but ν remains fixed, as l increases. However for larger l again the simple scaling of W breaks down in the range of <h> of 10^1-10^3 (Fig. 3). We reiterate that downward funneling to non-atop adsorption sites is the most realistic model of deposition dynamics. Thus, as temperature increases in MBE deposition processes, we expect the effective β to increase from the "low" EW value to higher "MBE values", and *not* to decrease from the unphysical value of 1/2.

The lack of simple scaling for W in models B and C with larger l reflects competition between various linear and non-linear terms driving the evolution. This behavior is perhaps not surprising since large terraces with multilevel steps can develop on these rough growing surfaces (see Fig. 4 and Ref.2). Our results show that the introduction of a large correlation length determined by l does not wash out the effects of adsorption site geometry and deposition dynamics (which would lead to recovery of simpler SOS behavior).

4. DISCUSSION AND EXPECTED BEHAVIOR FOR d=2+1.

In summary, the d=1+1 MBE model results for the SOS geometry of $\beta = 1/2$, when T = 0 K ($l = 0$) and $\beta = 3/8$ for kink mobility ($l \geq 1$) are modified if one incorporates realistic adsorption site geometries and deposition dynamics. Instead for T = 0 K ($l = 0$), one finds an EW value of β=1/4 for d=1+1 downward-funneling MBE models, and KPZ value of β=1/3 for d=1+1 random deposition MBE models. This follows from standard scaling arguments. Introducing kink mobility leads to smoothly increasing values of the effective β with increasing l. However for larger l,

the simple scaling of W breaks down in the range <h> of 10^1-10^3, so β values are less meaningful. This breakdown is associated with the development of rough surfaces with large terraces and multilevel steps.

In elucidating the behavior described above, it is instructive to compare the behavior of different types of models incorporating various degrees of: (i) downward mobility; (ii) mobility to kink sites as above; (iii) intralayer mobility only. For (i), ν increases strongly with increasing downward mobility for both SOS and bridge-site geometries (9). This is clearly reflected in the scaling behavior of W (9,10). For (ii), ν should not change significantly with increasing mobility to kink sites (which introduces no strong downward flux). Thus ν should remain (near) zero for SOS geometries and nonzero otherwise. However, κ_{eq} should increase strongly with mobility to kink sites. For sufficiently large l, this increase means that the quartic terms in Eq. 1 will dominate any quadratic terms of models B and C (at least for some range of <h>). This causes complicated behavior of W. For (iii) in SOS geometries, there is clearly no change in the Poisson column height statistics of the zero-mobility model, so $\nu = 0$ and $\beta = 1/2$ values are preserved.

One interesting feature of our results for d=1+1 MBE models B and C is that thick films with <h> =O(10^3) become rougher with increased mobility to kink sites. This is not the case for downward mobility. However mobility to kink sites facilitates clustering which generates more higher layer adsorption sites, as well as allowing migration to lower layers. Thus the net effect is unclear (11). Indeed there exist systems where increased mobility leads to rougher films (12).

Finally we comment on corresponding d=2+1 MBE models. In the SOS geometry, as l becomes non-zero, β should drop from 1/2 to 1/4 if the linear equation (4) applies (3), or to 1/5 if the non-linear quartic terms are significant (6). For low mobility d=2+1 MBE models with random deposition at (downward funneling to) four-fold follow (4fh) sites, say, one expects (1,13) a KPZ -value of β=1/4 (an EW-value of β=0, i.e., $W^2 \sim \log \langle h \rangle$). For larger l, β will presumably shift

towards the SOS value. Detailed studies are needed to determine if simple scaling behavior breaks down over the experimentally relevant range.

ACKNOWLEDGMENTS.

This work was supported by National Science Foundation Grant No. CHE-9014214, and was performed at Ames Laboratory. Ames Laboratory is operated for the U.S. Department of Energy by Iowa State University, under Contract No. W-7405-Eng-87. J.W.E. also acknowledges affiliation with the Department of Physics and Astronomy, Iowa State University.

Table 1. Dependence of the effective β on l for d=1+1 MBE models B and C for <h> in a range between about 10^2 and 10^3.

l	0	1	5	10	15-20
Model B	0.33	0.33	0.39	0.41	-
Model C	0.25	0.25	0.26	0.34	0.37

REFERENCES.

1. T. Vicsek, "Fractal Growth Phenomena" (World Scientific, Singapore, 1989); F. Family, Physica A 168, 561 (1990); J. Krug and H. Spohn, in "Solids Far from Equilibrium: Growth, Morphology, and Defects", edited by C. Godreche (Cambridge University Press, Cambridge, 1991).

2. D. E. Wolf and J. Villain, Europhys. Lett. 13, 389 (1990).

3. S. Das Sarma and P. Tamborenea, Phys. Rev. Lett. 66, 325 (1991).

4. J. W. Evans, D. E. Sanders, P. A. Thiel and A. E. De Pristo, Phys. Rev. B 41, 5410 (1990); D. E. Sanders and J. W. Evans, in "Structure of Surfaces III" edited by S. Y. Tong et al (Springer, Berlin, 1991); J. W. Evans, Vacuum, 41, 479 (1990), Phys. Rev. B 43, 3897 (1991).

5. J. Villain, J. Physique I 1, 19 (1991); L. -H. Tan and T. Natterman, Phys. Rev. Lett. 66, 2899 (1991).

6. Z. -W. Lai and S. Das Sarma, Phys. Rev. Lett. 66, 2348 (1991).

7. W. W. Mullins, in "Metal Surfaces: Structure, Energetics and Kinetics" (Am. Soc. Metal, Metals Park, Ohio, 1963).

8. J. Krug, J. Phys. A 22, L769 (1989).

9. H. C. Kang and J. W. Evans, Phys. Rev. A 44, 2335 (1991).

10. F. Family, J. Phys. A 19, L441 (1986).

11. J. W. Evans, D. K. Flynn and P. A. Thiel, Ultramicroscopy 31, 80 (1989).

12. R. Kunkel, B. Poellsema, L. K. Verheij and G. Comsa, Phys. Rev. Lett. 61, 733 (1990).

13. H. C. Kang and J. W. Evans, Surf. Sci. (to be submitted).

Figure Captions.

Figure 1. Schematic of d=1+1 MBE models incorporating migration to nearby kink sites immeadiately following deposition for: (a) random deposition in an SOS geometry; (b) random deposition at bridge sites; (c) downward funneling to bridge sites. Where trajectories split, one direction is chosen at random.

Figure 2. W versus <h> for the d=1+1 MBE model B (incorporating random deposition at bridge sites). Various l values are indicated.

Figure 3. W versus <h> for the d=1+1 MBE model C (incorporating downward funneling to bridge sites). Various l values are indicated.

Figure 4. A section of the growing interface for MBE model B with l=50 and h=4000.

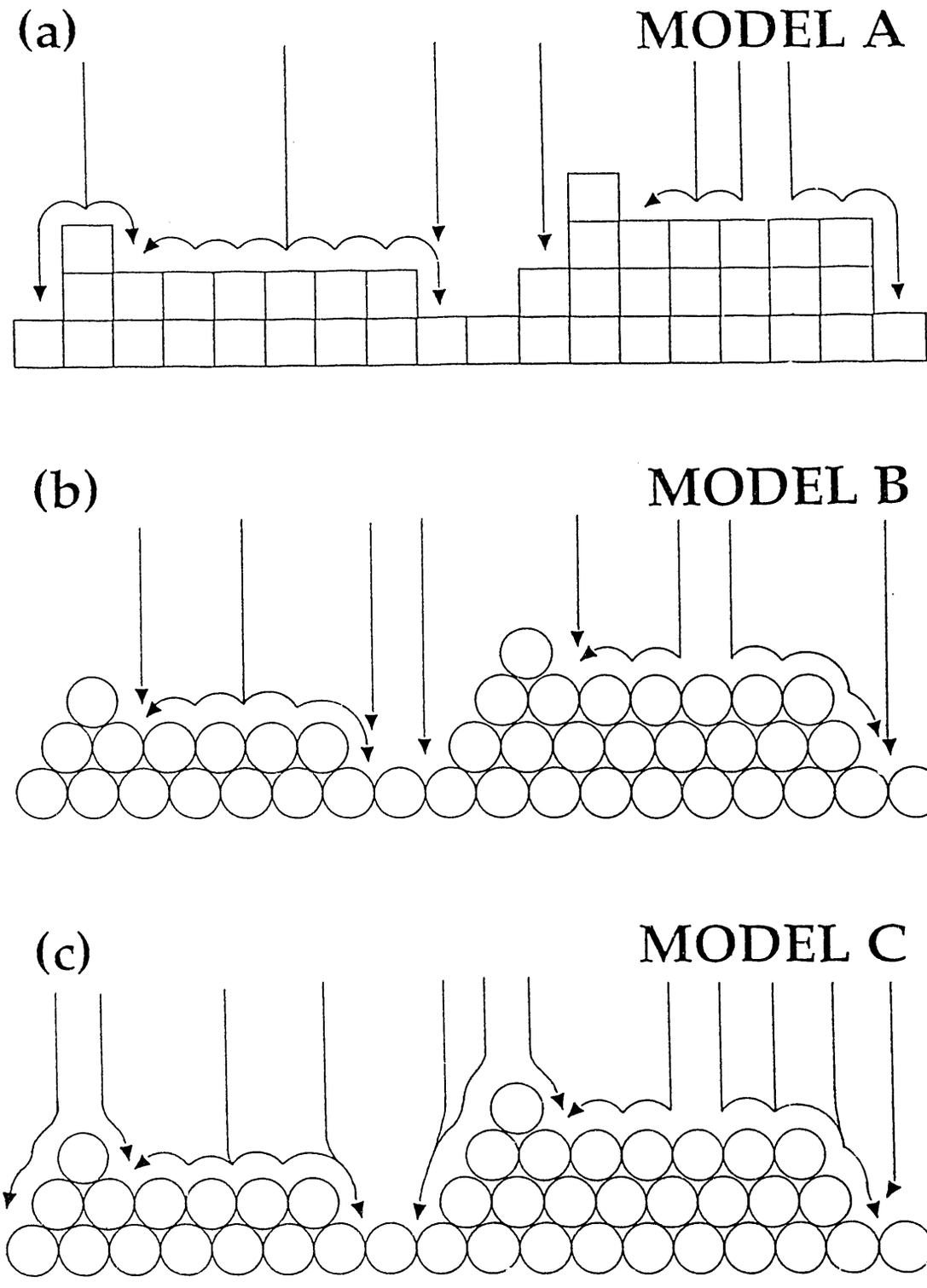

FIG. 1.

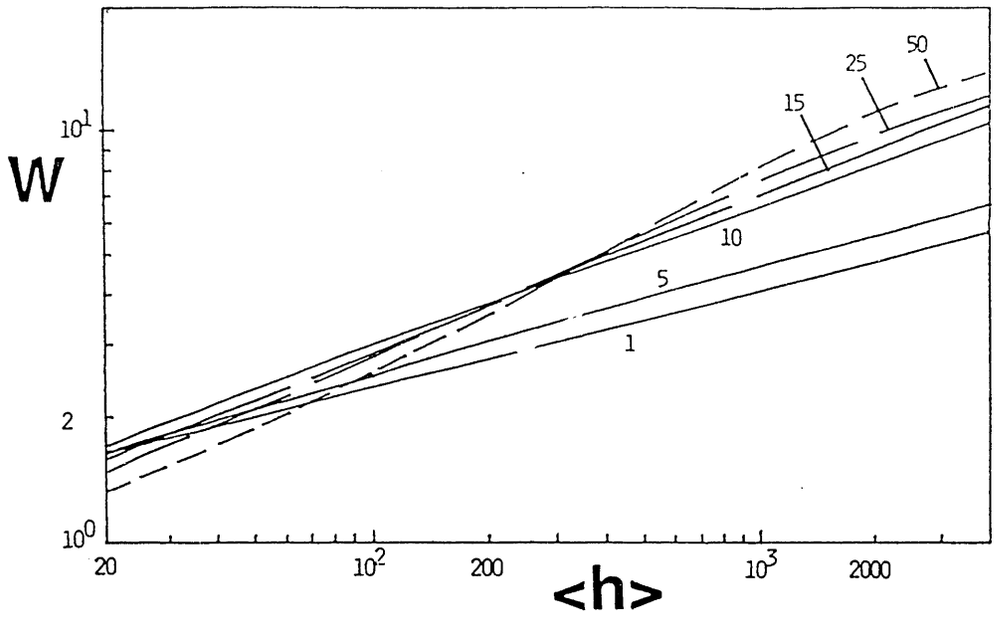

FIG. 2

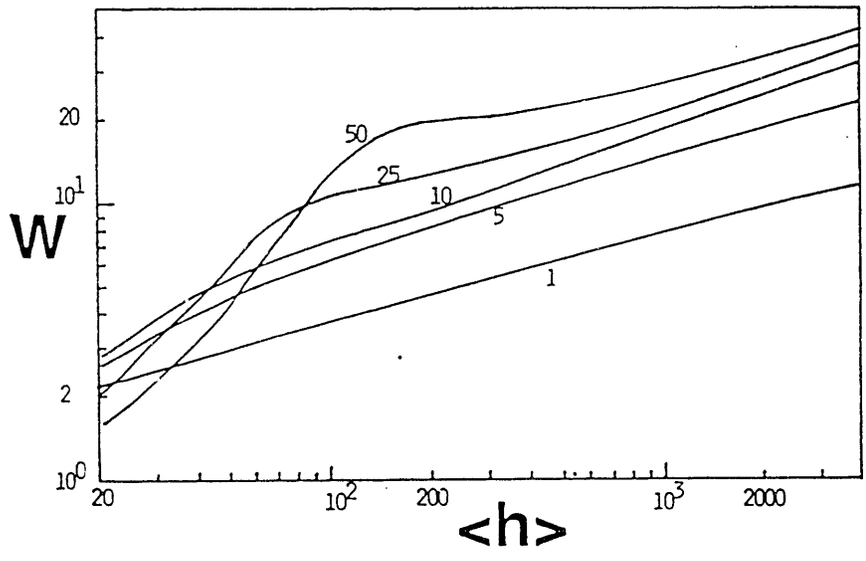

FIG. 3

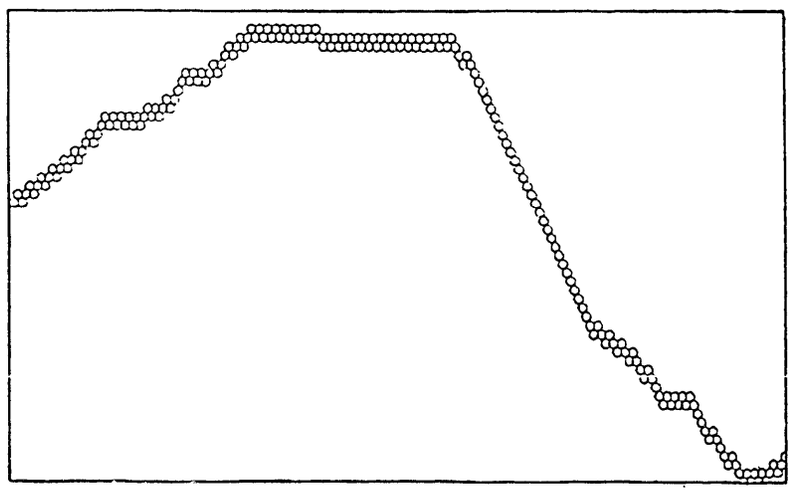

FIG. 4

END

DATE FILMED

12/26/91